Nanofibrous Membranes Prepared by Multiwalled Carbon Nanotube/ Poly(methyl methacrylate) Composites

Jun Hee Sung, Hyun Suk Kim, Hyoung-Joon Jin,* Hyoung Jin Choi, and In-Joo Chin

Department of Polymer Science and Engineering, Inha University, Incheon 402-751, Korea

Received August 10, 2004; Revised Manuscript Received October 3, 2004

ABSTRACT: Poly(methyl methacrylate) (PMMA) nanocomposites containing well-dispersed multiwalled carbon nanotubes (MWNTs) were prepared via an in-situ bulk polymerization of methyl methacrylate (MMA) in the presence of carbon nanotubes (CNTs). Electrical conductivities of the synthesized PMMA/MWNT nanocomposite films containing 1−5 wt % of MWNT were between 10^{-4} and 10^{-2} S/cm. When PMMA/MWNT nanocomposites with the same MWNT concentrations were electrospun in DMF into nanofibrous membrane, the conductivities were reduced to $\sim 10^{-10}$ S/cm, even though dispersion of the MWNTs in the electrospun nanofibers was superior to the conventional polymer composites with carbon nanotubes. The diameter of the electrospun fibers ranged between 120 ± 30 and 710 ± 20 nm. In addition, MWNTs in the electrospun nanofibers were found to be embedded in the polymer matix and to align along the fiber axis.

Introduction

Carbon nanotubes (CNT) possess remarkable electrical and mechanical properties coupled with good chemical stability due to their unique nanostructures.[1−3] Thus, polymer composites reinforced with CNTs are considered to have many engineering potentials, ranging from battery electrodes and electronic devices to much stronger composites.

Electronic properties of the perfect MWNTs are known to be similar to those of the single-walled CNTs (SWNTs) due to the one-dimensional electronic structure and the electronic transport characteristics. Several sheets of graphite are rolled up into tubes to form MWNTs, with the ends closed off by caps of various shapes. The MWNTs are made up of a series of cylinders nesting one inside the other like Russian dolls.[4] Since the CNTs are extremely flexible and possess high aspect ratio, it is extremely difficult to align and disperse the CNTs by using the ordinary composite fabrication methods. CNTs generally form stabilized bundles due to van der Waals force, resulting in the formation of hollow ropes. Therefore, obtaining a good dispersion of CNTs is known to be one of the key issues in using CNTs in composites.[5,6] By introducing small amounts of CNTs in the form of small bundles or individual tubes, mechanical strength, electrical conductivity, and thermal conductivity of the polymer composites can be improved tremendously compared with those of pristine polymer.[7−10] Dispersion of CNT in the polymer matrix has been studied from different points of view by noncovalent and by covalent functionalization as well.[11−13] In particular, MWNT can be functionalized and grafted with polymer chains via atom transfer radical polymerization, which can possibly control the molecular weight and its distribution within the resulting polymer.[14] Recently, to obtain homogeneous and fine dispersion of CNTs in the polymer matrix, Park et al.[15] adopted in-situ polymerization of methyl methacrylate (MMA) monomer containing functionalized MWNTs by a radical initiator. They observed that MWNTs were more uniformly dispersed in the PMMA matrix than in a composite simply prepared by using a PMMA solution and reported that successful dispersion of MWNT in PMMA resulted from the grafting of PMMA onto the CNT surface.

On the other hand, electrospinning is a fast and simple process driven by the electrical forces on the surface of the polymeric fluids, producing polymer filaments of nanoscale diameters.[16−21] Recently, it has been reported that the chemically functionalized CNTs in electrospinning process enhance various physical properties through modulating the interfacial interaction with the polymer matrix.[22−24]

In this work, MWNTs were embedded and aligned in PMMA nanofibers via an electrospinning process. The dispersion characteristics were improved via a bulk polymerization of PMMA in the presence of MWNTs. Unlike previous works on electrospinning of simple blends of CNTs with polymeric materials,[23] we incorporated CNTs as nanoscale fillers by in-situ polymerization of MMA. Thereby, we were able to disperse CNTs very well in the PMMA matrix prior to the electrospinning. We also investigated morphology and electrical conductivity of the electrospun PMMA nanofibers containing aligned MWNTs.

Experimental Section

Preparation of PMMA/MWNT Nanocomposites. The MWNTs (purity of 97%, supplied by Iijin Nanotec Co., Korea) synthesized by the thermal chemical vapor deposition were used in this study. To remove metallic catalysts from MWNTs prior to use the MWNTs were treated in 3 M HNO_3 at 60 °C for 12 h and then in 5 M HCl at 120 °C for 6 h.[25] The purity of the treated MWNT was measured to be 99% using thermogravimetric analysis. This acid treatment is known to introduce carboxyl and hydroxyl functional groups on MWNT, which render MWNT more compatible with common organic solvents.[26] Acid-treated MWNTs were then dispersed in MMA monomer for 5 h at 25 °C using a ultrasonic generator (Kyungil Ultrasonic Co., Korea), which has a nominal frequency of 28 kHz at 600 W. Bulk polymerization of MMA (20 g) in the presence of dispersed MWNTs was performed at 60 °C with

* Corresponding author: Tel +82-32-860-7483; Fax +82-32-865-5178; e-mail hjjin@inha.ac.kr.

10.1021/ma048355g CCC: $27.50
Published on Web 12/02/2004

2,2′-azobis(isobutyronitrile) (AIBN) (0.04 g) as an initiator in a capped glass test tube. PMMA/MWNT composites thus prepared showed MWNT contents of 0, 1, 3, and 5 wt % with respect to MMA. After polymerization, the MWNT/PMMA composites were separated from test tubes and characterized by a Fourier transform infrared spectrometer (FT-IR, Perkin-Elmer, Spectrum 2000) to evaluate the chemical structure using a KBr pellet.

Electrospinning Process. To prepare a sample solution for the electrospinning process, the PMMA/MWNT composite obtained from in-situ polymerization of MMA was dissolved in dimethylformamide (DMF) for 2 days. The solution concentration of the PMMA/MWNT composites in DMF varied with the MWNT content in composites: 4.0 wt % both for PMMA only and for 1 wt % MWNT content, 4.7 wt % for 3 wt % MWNT content, and 5 wt % for 5 wt % MWNT content in PMMA/MWNT composites. The higher the MWNT content in the PMMA/MWNT composites, the higher the solution concentration for the electrospinning.

The electrospinning appratus was composed of several components: a high-voltage supplier (Gamma High Voltage Research, E3 30P-5W), a capillary tube with a stainless steel needle (16 gauge), a syringe pump (Harvard Apparatus), and a stainless steel collecting screen (diameter ≈ 10 cm) as described elsewhere.[21,27,28] A high electric field from the high-voltage supplier is generated between the needle and the collection plate. As it reaches a certain voltage difference, the electrical charge passing through the polymer solution overcomes surface tension of the polymer solution droplet that is formed at the tip of the needle. Electrospinning was carried out using a syringe with a 1.2 mm diameter spinneret at an applied voltage difference of 30 kV over the distance of 50 cm ($E = 0.6$ kV/cm). As the MWNT content was increased, DMF was evaporated more slowly, resulting in great difficulty in producing uniform fibers. The distance between the needle and the collector had to be kept much farther compared to other systems where the typical distance is 15−20 cm. Prior to electrospinning, the solution of PMMA/MWNT in DMF was sonicated for 1 h to obtain homogeneous dispersion. The syringe pump was set to deliver the solution at a flow rate of 10 μL/min using a 5 mL syringe.

Characterization of PMMA/MWNT Composites and Electrospun Nanofibers. The amount of MWNT dispersed in PMMA/MWNT composites was examined by thermogravimetric analysis (TGA) (Q50, TA Instrument). The surface morphology and the fiber shape were observed via a field emission scanning electron microscope (FESEM, S-4300, Hitachi, Japan), and the orientation of MWNT in the PMMA/MWNT nanofibers was characterized using a transmission electron microscope (TEM) (CM 200, Philips, The Netherlands). The solution shear viscosity was measured via a rotational rheometer (MCR-300, Paar-Physica, Germany) equipped with a concentric cylinder-type measuring unit. The electrical conductivity of electrospun nanofibers of the PMMA/MWNT composites was measured by a four-probe method with a high-voltage source measurement unit (237 Keithley).

Results and Discussion

Figure 1 shows TGA curves of the PMMA/MWNT composites with various concentrations of MWNTs, at a heating rate of 20 °C/min with N_2 gas purging. When it was heated to 900 °C, more residues were observed for higher MWNT contents. PMMA starts to degrade around 200 °C and completely decomposes at 400 °C. The PMMA/MWNT composites also decomposed at 400 °C, and the amount of MWNT in the composite remained at higher temperatures.

The molecular weights of PMMA in the PMMA/MWNT nanocomposites with different CNT contents are described in Table 1, showing that the molecular weight of PMMA increases with the MWNT content due to its participation in the polymerization resulting from consuming AIBN.[9] AIBN can initiate the polymerization

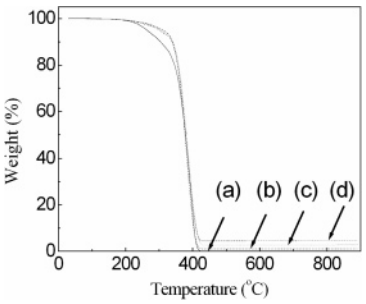

Figure 1. TGA thermograms of (a) PMMA and PMMA/MWNT composites: (b) 99/1, (c) 97/3, and (d) 95/5 wt %.

Table 1. Molecular Weights of PMMA in PMMA/MWNT (wt %) Composites by GPC

PMMA/MWNT	100/0	99/1	97/3	95/5
M_w	311100	447300	613600	741400
M_n	72800	110500	166500	217800
PI[a] (M_w/M_n)	4.27	4.05	3.68	3.40

[a] Polydispersity index.

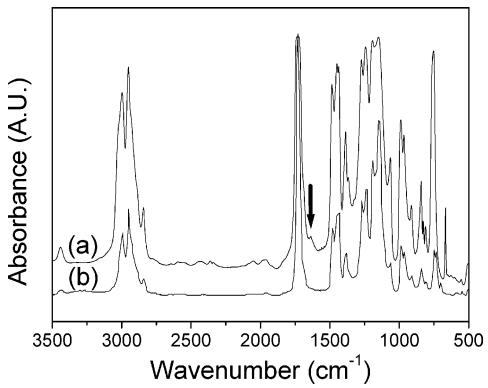

Figure 2. FT-IR spectrum of (a) PMMA/MWNT (99/1 wt %) composite and (b) pure PMMA.

of MMA monomers in the bulk. Also, AIBN is capable of opening the π-bonds of CNTs, and the generation of radicals on MWNT surface by the AIBN triggers the growth of PMMA chains tethered on the CNT surface, resulting in the increase in the molecular weight of PMMA.[15] The molecular weights shown in Table 1 are the ones of the PMMA chains that are free from the CNT surface because the chains adsorbed onto the CNT were filtered out prior to the GPC measurement. The additional consumption of AIBN led to a reduction in the number of radicals during the reaction and eventually an increase in the PMMA molecular weight.

Chemical structures of the composites of MWNT and PMMA as well as pristine PMMA were further analyzed by an FT-IR spectrometer (Figure 2). A new peak at 1650 cm^{-1} (the arrow in Figure 2) was observed in the composites. It is believed to be originated from a C−C bond between MWNT and PMMA, which was formed during polymerization initiated by the radicals on the surface of MWNT.[9,15]

Figure 3 shows the nonwoven membranes formed by the electrospun nanofibers of both PMMA/MWNT and PMMA from the DMF solutions. They display quite compact textures over a large area. The color of the electrospun mat was gray due to the presence of the MWNTs embeded in the nanofibers.

Figure 4 displays SEM photographs of the electrospun nanofibers of PMMA/MWNT composites. The electrospun nanofibers of PMMA/MWNT composites show a

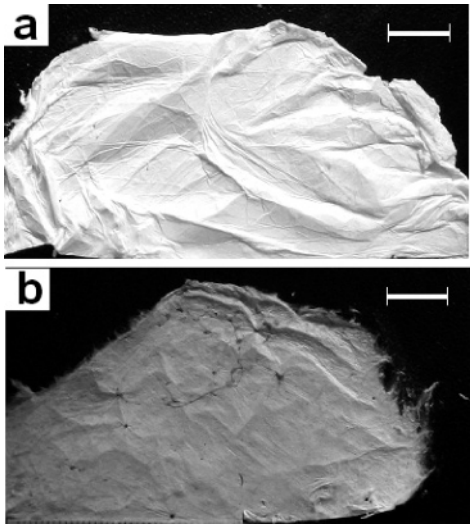

Figure 3. Membrane images of electrospun nanofibers of (a) pure PMMA and (b) PMMA/MWNT (97/3 wt %). Scale bars: 10 mm.

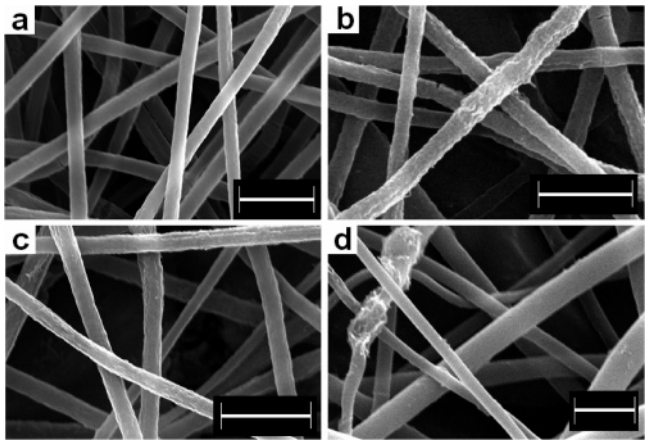

Figure 4. SEM images of electrospun nanofibers of PMMA/MWNT composites: (a) pure PMMA (b) 99/1, (c) 97/3, and (d) 95/5 wt %. Scale bars: 2 μm.

relatively broad size distribution (fiber diameter: about 100−700 nm) with different MWNT contents compared with that of the electrospun PMMA without MWNT (520 ± 50 nm, $N = 50$). The surface of the PMMA electrospun nanofibers without MWNT is very smooth, as shown in Figure 4a. On the other hand, addition of the CNTs into PMMA made the fiber surface rough and uneven, while the MWNTs were well embedded in the fiber (Figure 4b,c). As the CNT content increased, the electrospun nanofibers showed some aggregates and local irregularities, as shown in Figure 4d. It was rather difficult to spin the PMMA/MWNT solution containing 5 wt % CNT due to its higher solution viscosity with a larger shear thinning behavior compared with other solutions in Figure 5. Although the shear viscosity of the PMMA/MWNT solution increased with the MWNT content, high solution concentration was required to electrospin the PMMA/MWNT solution with higher MWNT content. It is due to the fact that as the MWNT content in the solution increases, the elasticity of the solution decreases, thus making the electrospinning rather difficult.

SEM images in Figure 6 show various types of surface irregularities of the nanofibers in detail. It is clearly shown that some parts of the CNT are knotted or entangled or protruded from the side or from the end

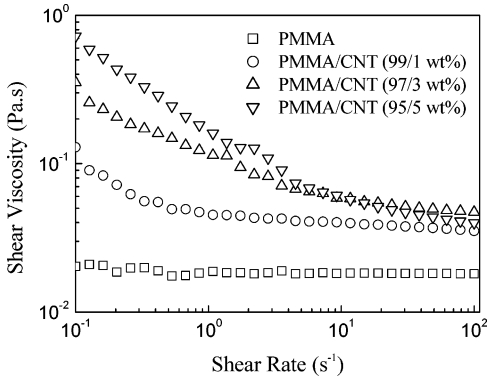

Figure 5. Shear viscosity of PMMA/MWNT composites with different MWNT contents in DMF.

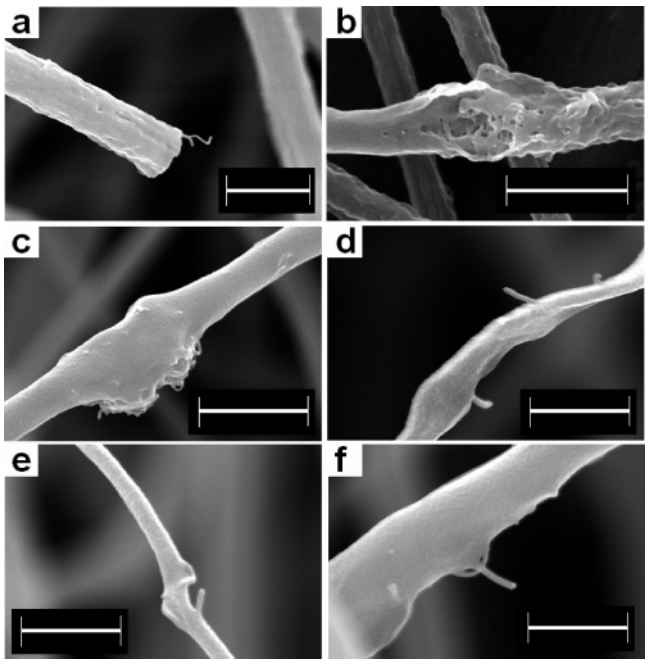

Figure 6. SEM images of electrospun nanofibers of PMMA/MWNT showing several types of irregularities: (a, b) PMMA/MWNT (99/1 wt %); (c−f) PMMA/MWNT (95/5 wt %). Scale bars: 1 μm for (a−c) and 500 nm for (d−f).

of the nanofibers. Note that SWNT bundle protruding from the edge is also recently reported for SWNT−polyurethane nanofibers.[20]

We further investigated the internal structural details of the PMMA/MWNT electrospun nanofibers containing different amounts of CNT by TEM. Figure 7 compares TEM images with SEM images of the embedded CNTs that are well-oriented along the nanofiber axis. In Figure 7a, the TEM photograph clearly shows that the embedded CNTs are entangled, even though the solution viscosity of the PMMA/MWNT containing 1 wt % MWNT was lower than other solutions containing higher MWNT contents. However, it should be noted that the carbon nanotube appears well dispersed within the nanofiber individually. The electrospun nanofibers with the CNT content of 3 wt %, shown in Figure 7b,c, were well aligned and almost fully extended. However, as the CNT content in PMMA increased to 5 wt %, the surface of some fibers was irregular and rough due to aggregation of the CNT during the electrospinning process (Figure 7d). Figure 7d compares TEM images with SEM images. Even though the MWNTs are considered to be well oriented, partially bent and twisted

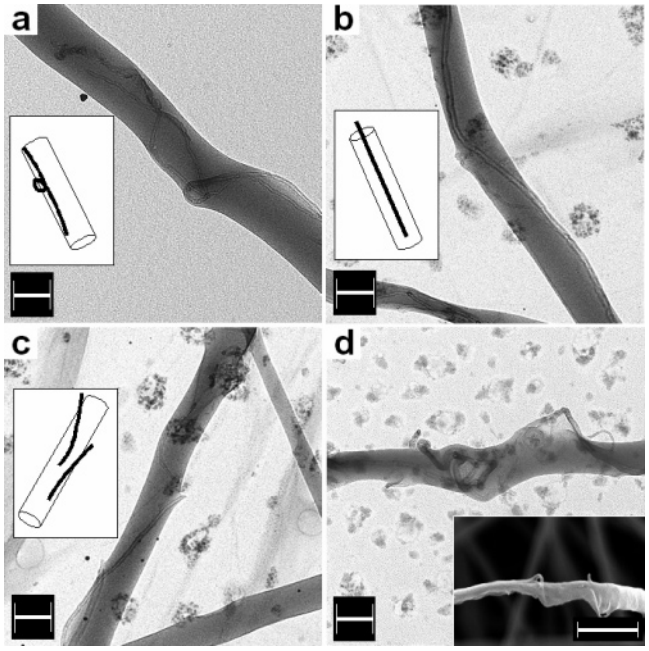

Figure 7. TEM images of electrospun nanofibers of PMMA/MWNT composites: (a) 99/1, (b) and (c) 97/3, and (d) 95/5 wt %. Scale bars: 100 nm for (a−c), 200 nm for (d), and 1 μm for SEM image in (d).

CNTs within nanofibers are also shown. The diameter of nanofibers was affected by the degree of the MWNT alignment within the nanofibers. Nanofiber diameter can be further controlled by the processing condition. As confirmed in Figure 7, the embedded CNTs within the nanofibers could be identified, and their alignments could also be investigated by SEM and TEM images.

Because the CNTs are electrically conductive, it was interesting to monitor electrical conductivities of PMMA/MWNT bulk films and the electrospun PMMA/MWNT nanofibrous membranes. The PMMA/MWNT films were prepared by solvent casting with a film thickness of 150 μm. The electrical conductivity of PMMA/MWNT (99/1 wt %) film was 3.1×10^{-4} S/cm, and that of PMMA/MWNT (95/5 wt %) films was 1.4×10^{-2} S/cm, while the electrical conductivity of pure PMMA film was very low at 10^{-14}−10^{-15} S/cm. However, electrical conductivity of the electrospun PMMA/MWNT membrane was found to be approximately $\sim 10^{-10}$ S/cm, regardless of the MWNT concentration.

It should be noted that the physical state of the PMMA/MWNT composite affects the electrical conductivity at the same MWNT loading, although there was a report that in-situ polymerization in the presence of the CNTs could induce some defects on the CNT surface.[11] In the case of electrospun nanofibrous membranes of PMMA/MWNT, both the high porosity of the nonwoven membranes[29] and the fact that the PMMA chains wrapped around the MWNTs in individual PMMA/MWNT nanofibers may have contributed to lowering of electrical conductivity.

Conclusions

We prepared the PMMA/MWNT composites by effectively dispersing MWNTs via an in-situ bulk polymerization of MMA. Electrospinning of the composite solution produced nanofibrous membranes with well-aligned and embedded CNTs within individual fibers, as observed by SEM and TEM. The electrical conductivity of the electrospun PMMA/MWNT composite membranes was lower that that of the bulk composite film at the same concentration of MWNTs. Not only high porosity of the electrospun membrane but also excellent wrapping of PMMA chains around the MWNT may have caused the reduction of electrical conductivity. It was found that the electrospinning process was a useful method for aligning the CNTs in the nanofibers but not very efficient for enhancing electrical conductivity of matrix polymer.

Acknowledgment. H.J.C. acknowledges the research grant from the ARC, Korea (2004). This work was supported by the Korea Research Foundation Grant (KRF-2003-003-D00103). We thank S. J. Park for technical input.

References and Notes

(1) Iijima, S. *Nature (London)* **1991**, *354*, 56−58.
(2) Ishikawa, H.; Fudetani, S.; Hirohashi, M. *Appl. Surf. Sci.* **2001**, *178*, 56−62.
(3) Lillehei, P. T.; Park, C.; Rouse, J. H.; Siochi, E. J. *Nano Lett.* **2002**, *2*, 827−829.
(4) *Carbon Nanotubes and Related Structures: New Materials for the 21st Century*; Harris, P. J. F., Ed.; Cambridge University Press: New York, 1999; Chapter 3.
(5) Bower, C.; Rosen, R.; Jin, L.; Han, J.; Zhou, O. *Appl. Phys. Lett.* **2000**, *77*, 663−665.
(6) Amelinckx, S.; Bernaerts, D.; Zhang, X. B.; Van Tendeloo, G.; Van Landyt, J. *Science* **1995**, *267*, 1334−1338.
(7) Qin, S.; Qin, D.; Ford, W. T.; Resasco, D. E.; Herrera, J. E. *J. Am. Chem. Soc.* **2004**, *126*, 170−176.
(8) Sreekumar, T. V.; Liu, T.; Min, B. G.; Guo, H.; Kumar, S.; Hauge, R. H.; Smalley, R. E. *Adv. Mater.* **2004**, *16*, 58−61.
(9) Jia, Z.; Wang, Z.; Xu, C.; Liang, J.; Wei, B.; Wu, D.; Zhu, S. *Mater. Sci. Eng.* **1999**, *A271*, 395−400.
(10) Regev, O.; Elkati, P. N. B.; Loos, J.; Koning, C. E. *Adv. Mater.* **2004**, *16*, 248−251.
(11) Kamaras, K.; Itkis, M. E.; Hu, H.; Zhao, B.; Haddon, R. C. *Science* **2003**, *301*, 1501.
(12) Chen, J.; Hamon, M. A.; Hu, H.; Chen, Y.; Rao, A. M.; Eklund, P. C.; Haddon, R. C. *Science* **1998**, *282*, 95−98.
(13) Tang, B. Z.; Xu, H. *Macromolecules* **1999**, *32*, 2569−2576.
(14) Kong, H.; Gao, C.; Tan, D. *Macromolecules* **2004**, *37*, 4022−4030.
(15) Park, S. J.; Cho, M. S.; Lim, S. T.; Choi, H. J.; Jhon, M. S. *Macromol. Rapid Commun.* **2003**, *24*, 1070−1073.
(16) Yarin, A. L.; Koombhongse, S.; Reneker, D. H. *J. Appl. Phys.* **2001**, *90*, 4836−4846.
(17) Fong, H.; Chun, I.; Reneker, D. H. *Polymer* **1999**, *40*, 4585−4592.
(18) Baumgarten, P. K. *J. Colloid Interface Sci.* **1971**, *36*, 71−9.
(19) Doshi, J.; Reneker, D. H. *J. Electrostat.* **1995**, *35*, 151−60.
(20) Shin, Y. M.; Hohman, M. M.; Brenner, M. P.; Rutledge, G. C. *Appl. Phys. Lett.* **2001**, *78*, 1149−1151.
(21) Shin, Y. M.; Hohman, M. M.; Brenner, M. P.; Rutledge, G. C. *Polymer* **2001**, *42*, 9955.
(22) Ko, F.; Gogotsi, Y.; Ali, A.; Naguib, N.; Ye, H.; Yang, G.; Li, C.; Willis, P. *Adv. Mater.* **2003**, *15*, 1161−1165.
(23) Sen, R.; Zhao, B.; Perea, D.; Itkis, M. E.; Hu, H.; Love, J.; Bekyarova, E.; Haddon, R. C. *Nano Lett.* **2004**, *4*, 459−464.
(24) Dror, Y.; Salalha, W.; Khalfin, R. L.; Cohen, Y.; Yarin, A. L.; Zussman, E. *Langmuir* **2003**, *19*, 7012−7020.
(25) Velasco-Santos, C.; Marínez-Hernández, A. L.; Lozada-Cassou, M.; Alvarez-Castillo, A.; Castaño, V. M. *Nanotechnology* **2002**, *13*, 495−498.
(26) Liu, J.; Rinzler, A. G.; Hafner, J. H.; Bradley, R. K.; Boul, P. J.; Lu, A.; Shelimov, K.; Huffman, C. B.; Rodriguez-Macias, F.; Shon, Y. S.; Lee, T. R.; Colbert, D. T.; Smalley, R. E. *Science* **1998**, *280*, 1253−1256.
(27) Jin, H.-J.; Fridrikh, S. V.; Rutledge, G. H.; Kaplan, D. L. *Biomacromolecules* **2002**, *3*, 1233−1239.
(28) Wang, M.; Jin, H.-J.; Kaplan, D. L.; Rutledge, G. C. *Macromolecules* **2004**, *37*, 6856.
(29) Norris, I. D.; Shaker, M. M.; Ko, F. K.; MacDiarmid, A. G. *Synth. Met.* **2000**, *114*, 109−114.

MA048355G